Self-healing epoxy via epoxy-amine chemistry in dual hollow glass bubbles

He Zhang, Pengfei Wang, Jinglei Yang*

School of Mechanical & Aerospace Engineering, Nanyang Technological University, Singapore

*Corresponding author. Email: MJLYang@ntu.edu.sg, Tel: +65 6790 6906

Abstract

Etched hollow glass bubbles (HGBs) with through-holes at micron level were used as micro-containers for epoxy and amine solution to realize the self-healing functionality in epoxy matrix. The average diameter, the average shell thickness, as well as the cavity inside the shell were investigated. In order to check the mechanical robustness and the rupturability of the HGBs, micro-compression tests of single HGB were conducted to measure their mechanical responses, which reveal the relatively high compressive strength and brittle feature. A new type of self-healing epoxy was developed based on the dual HGB carriers and the self-healing performance was optimized systematically to obtain better healing behavior. It is found the highest healing efficiency of about 62% was achieved at 50 °C for 24 h when 12.5 - 15.0 wt% healing agent carriers was incorporated at the optimized ratio of 4 : 1 for epoxy loaded HGBs (HGB-E) to amine loaded HGBs (HGB-A). It is also found that the healing efficiency increased with increased healing duration at 50 °C. In addition, the fracture toughness is improved and the tensile modulus keeps constant while the tensile strength is deteriorated by the incorporation of the carriers.

Keywords: A. Smart materials; A. Self-healing epoxy; B. Fracture toughness; D. Fractography.

1. Introduction

As an extensively used engineering polymeric material, epoxy resin has drawn much attraction due to its excellent physical, chemical, as well as thermal properties. The wide range of applications for epoxy includes the functional coatings, the electronic/dielectric

components, structural adhesives, and most importantly the composites as the adhesive and protective matrix [1]. However, this thermoset with high cross-link density is very brittle, leading to its high sensitivity to in-born defects or force-induced cracks. Variety approaches have been proposed to improve the fragile feature of the epoxy resin, among which the incorporation of self-healing functionality [2-4] is very promising because of the toughening effect by the added healing agent carriers as micro-fillers [5] and the re-bonding of the induced micro-cracks timely upon their formation. Self healing in epoxy can be realized by various means in different scales, such as by layup of hollow tubes [6-12], fabrication of micro-vascular networks [13], microencapsulation [14-21], thermal additives [22], as well as molecular design by Diles-Alder reaction [23]. Attributed to the ease of manufacture and material integration, the embedment of microcapsules containing healants is the most popular approach among all the methods.

Nowadays, the homogeneous healing of epoxy with epoxy-hardener chemistry has been attracting more and more attention. Because epoxy monomers can be easily incorporated to the epoxy matrix by different methods, the embedment of hardeners into epoxy matrix is the key point for the homogeneous healing. Previously some secondary hardeners for epoxy, like latent curing agent [24], polymercaptan [16], and cationic catalyst [17, 18], have been adopted to realize the homogeneous healing in epoxy. Recently, the widely used amine and amine derivative hardeners were also encapsulated by various methods, including reverse emulsion method [25], solvent evaporation method [26], and loading by synthesized hollow poly(ureaformaldehyde) (PUF) microcapsules [27, 28]. However, the polymeric shell would be corroded by the highly corrosive amine during their service life and would be downgraded by the thermal treatment during manufacturing of the material and their application.

As epoxy is the most widely employed adhesive matrix in composites, it is also very exciting to incorporate the self-healing functionality into composite materials [6, 8, 12, 29-34].

Successful cases with good healing performance were reported via various self-healing approaches similar as in the pure epoxy matrix. Considering the much harsher processing conditions for composite materials, such as repeatedly brushing the adhesive, pressing to remove the excess amount of the adhesive, relatively high post heat-treatment temperature up to hundreds centi-degree, the carriers for the healing agents should be strong enough to survive from the manufacturing of the composites. Keller and Sottos [35] tested the elastic stiffness and the strength of the PUF shell, revealing that the microcapsules with smaller diameter have a higher normalized failure strength while failing at lower loads. Yang et al. [36] also tested the mechanical properties of the synthesized polyurethane (PU) microcapsule containing diisocyanate, finding that the PU shell is relatively brittle compared with the flexible feature possessed by the PUF shell. Although the higher strength of the carrier does not always mean better healing behavior considering the rupturability of the carrier at the crack plane upon the fracture event, the relatively higher strength of the carrier enables the higher survivability of the carriers. Combining with the corrosive feature of some healing agents and thermally degradability of the shell, to explore healing carriers with relatively higher strength, chemical inertness, as well as thermally stability, is one direction to advance the self-healing materials.

HGBs can be very attractive alternative carriers for healing agents considering their good mechanical properties, thermal stability up to thousand centi-degree, and excellent inertness to most chemicals. In our previous investigations, we have reported the etching of HGBs with diluted hydrofluoric acid (HF) using a specially designed reaction system and their applications as micro-containers for self-healing agents [37-39]. When the etched HGBs loaded with amine solution and the microcapsules containing epoxy solution were mixed into epoxy matrix, satisfactory healing performance was achieved in this system. However, the system is not good to be used in composites materials due to the difficulty of synthesizing

small epoxy microcapsules with good flowability and the relatively low mechanical strength of the PUF shell. In order to avoid the usage of epoxy microcapsules, we reported the fabrication of self-healing epoxy via both epoxy monomer and amine solution carried by etched HGBs.

2. Experiment

2.1 Materials

Epoxy and related hardener, Epolam 5015 (ρ_{5015} = 1.150 g/cm^3) and hardener 5015, were purchased from Axson. Neopentyl glycol diglycidyl ether (NGDGE, ρ_{NGDGE} = 1.04 g/cm^3) as the reactive diluents for epoxy, diethylenetriamine (DETA, ρ_{DETA} = 0.951 g/cm^3), 2,4,6-tris(dimethylaminomethyl)phenol (DMP 30, ρ_{DMP} = 0.969 g/cm^3) as the epoxy curing accelerator, acid yellow 73 as the color indicator, were ordered from Sigma Aldrich. HGBs were bought from 3M. All the chemicals were used as received from the supplier.

2.2. Etching of HGBs

The adopted HGBs with through-holes were etched using a specially designed reaction system, as reported in our previous report [37]. Sieved HGBs with diameter from 63 - 90 μm were first water-deposited to remove the debris. 2 g HGBs, enough deionized (DI) water, were charged into the container while 160 ml etching agent, 1% diluted HF solution, was charged into the feeder. Under stirring at 45 rpm, the HF solution was added into the mixture in the container at feeding rate of about 35 - 40 drops/min. After about 12 h, the process was ceased, and the etched HGBs depositing at the bottom zone were collected. In order to completely remove the free fluorochemicals in the collection, the HGBs were rinsed with DI water for 3 - 4 times. The HGBs were dried at room temperature (RT~ 20 °C) for 24 h and water-deposited again using a separation funnel to remove the debris. The process was repeated for 3 - 4 times for better quality. Finally, the floating HGBs in the separation funnel were collected and dried at RT for 24 h as the target product.

2.3. Mechanical characterization of the collected HGBs

The compressive properties of the etched HGBs with through-holes were conducted using single microsphere compression apparatus as reported by Keller and Sottos [35], and Yang et al. [36]. The schematic configuration can be found in the inset in Figure 2a. The employed loading rate for the stepper actuator (Physik Insturmente M-230S) was 2 μm/s and was controlled by a computer. The load was recorded by a 0.5 N load cell (FUTEK). Images were taken prior the compression tests to measure the diameter of the HGBs.

Before tests, the HGBs were added into acetone solution in a 20 ml vial. One small drop of the mixture with several HGBs was transferred to the bottom of the compression rod. After the evaporation of acetone, extra HGBs were removed carefully to leave only one bubble at the end of the rod.

2.4. Loading of the HGBs with healants using the vacuum-assisted method

The vacuum-assisted device and related method for the loading with amine solution was illustrated in our previous report [37]. Briefly, firstly the HGBs were charged into a two-neck flask with one neck connected to a vacuum pump and another neck equipped with a separation funnel for the addition of amine solution. After 30 min's evacuation, the outlet was blocked and the amine solution, DETA with 10 wt% DMP 30, was fed in through the separation funnel. The system was hold for about 30 min for the full infiltration of amine solution into the cavity of the HGBs. And finally the HGBs with amine solution inside were separated by absorbing away the residual amine solution by tissues, and collected as the target product for further usage.

As the epoxy solution to be loaded, Epolam 5015 with 30 wt% NGDGE, is a little viscous, warm-up of the system and the solution to about 80 °C was executed to reduce the viscosity. Vacuum pump was employed to assist the removal of the residual epoxy solution outside.

The equivalent hydrogen weight (EHW), defined as the weight in grams that contains 1 mol equivalent of reactive hydrogen atom, is 22.89, based on the composition of the amine solution and the theoretical functionality of DETA (n = 5). The density of the loaded amine solution is 0.953 g/cm^3 based on the ratio of the gradients. According to the composition of Epolam 5015 [40] and ratio of each gradients, we can estimate that the equivalent epoxide weight (EEW), defined as the weight in grams that contains 1 mol equivalent of epoxide, of the loaded mixer is approximately 133. And the density of the epoxy solution is 1.117 g/cm^3.

2.5. Fabrication and assessment of the self-healing epoxy TDCB specimen

The self-healing behaviour of the epoxy resin incorporated with healing agent carriers could be characterized by the mode I fracture toughness using tapered double-cantilever beam (TDCB) specimen with localized short groove, as stated by Brown et al [41]. Epolam 5015, and the related hardener 5015, was mixed for about 5 min at the ratio recommended by the supplier, and further degassed for about 15 min to eliminate the trapped air-bubbles. Later, the epoxy loaded HGBs (HGB-E) and amine loaded HGBs (HGB-A) at different ratios and concentrations were dispersed into the mixture uniformly. The mixture was filled into the short groove of the TDCB specimens, cured at RT for 24 h, and further post-cured at 35 °C for another 24 h. In order to investigate the influence of healing time at 50 °C on the healing behaviour, one set of specimen was healed at 50 °C for certain duration.

The self-healing tests were carried out using an Instron testing machine (Instron Mini High Precision Tester). Before the fracture toughness testing, a pre-crack was introduced by a sharp razor. Loading speed of 1 mm/min was adopted for the overhead. After the fully fracture of the specimen along the middle plane at the short groove, the specimens were healed under various conditions at 50 °C for different durations. Healing tests were performed using the same machine under the same parameters. Herein, because of the same geometry of the TDCB specimens, the healing efficiency could be expressed as:

$$\eta = \frac{K_{IC}^{Healed}}{K_{IC}^{Original}} = \frac{P_C^{Healed}}{P_C^{Original}} \quad (1)$$

where η is the healing efficiency, K_{IC}^{Healed} and $K_{IC}^{Original}$ mean the healed fracture toughness and the original fracture toughness, respectively, and the P_C^{Healed} and $P_C^{Original}$ mean the healed peak load and original peak load, respectively.

2.6. Tensile property of the formulated self-healing epoxy

Tensile dog-bone specimens were fabricated and tested according to ASTM standard D638. The formulated pure epoxy or self-healing epoxy was added into rubber moulds for molding. The specimens were cured at RT for 24 h followed by another 24 h at 35 °C. The tensile testing was conducted using an Instron machine (Instron 5500R) with loading speed of 1 mm/min for the overhead. For the accurate measurement of the strain, an extensiometer (Instron, Static Extensiometer GL 25 mm) with gauge length of 25 mm was employed.

2.7. Characterization methods

The morphology, the size distribution, and the shell thickness of the collected original HGBs were imaged by the field emission scanning electronic microscopy (FESEM) (JOEL JSM-7600F). The diameter and the shell thickness of the HGBs were measured from the SEM images using the software ImageJ based on at least 100 individuals. The fracture surface after healing test was observed using the FESEM. The cavity of the original HGBs, as well as the loaded HGBs dispersed in the host, were characterized by the optical microscopy (Olympus CKX41) with florescent mode.

3. Result and discussion

3.1. Characterization of the HGB before and after etching

Figures 1a and 1b separately show the SEM images of the adopted original HGBs in the etching process and the morphology of the outer surface of the bubbles. It can be seen that a lot of glass nano-particles adhere to the smooth outer surface of the original HGBs. The inset

in Figure 1a at top right gives the typical shell thickness of the original HGBs. The measured diameter of this original HGB is 67.5 ± 7.4 μm, and the shell thickness is 1.16 ± 0.57 μm. Figure 1c shows the overview SEM image of the etched HGBs with through-holes after water-deposition to remove the debris and bubbles with relatively big holes. It is observed from the SEM image that very few through-holes at several microns can be found at every etched HGB. The enlargement at the bottom right in Figure 1c shows a typical etched HGB with small through-holes of about 2 μm. The inset in Figure 1c at top right indicates the typical shell thickness and the etched rough outer shell with many etching pits of the HGB. The measured diameter of the etched HGB is 66.9 ± 8.2 μm, and the shell thickness is 0.79 ± 0.41 μm. Figure 1d gives the optical microscopic image of the etched HGBs, which demonstrates that the cavity inside the glass shell is very clean without anything. The cleanness of the HGBs assures that they can carry as much healing agent as possible for self-healing purpose.

3.2. Mechanical properties of etched HGBs

Figure 2a describes the micro-compressive testing process of a single etched HGB right below the compressive rod (as indicated by the arrow). The inset in the figure shows the schematic configuration. The diameter of the tested HGBs was measured by comparing the diameter of the HGBs to the known diameter of the compressive rod (2 mm). Figure 2b gives a representative Load-Displacement curve for the testing in the diametral direction. The average peak load by testing several different HGBs is 4.91 ± 1.02 mN. And the measured maximum displacement relative to the diameter is 8.13 ± 1.11%, which is much lower than that the PUF microcapsule(~ 35% for 63 μm) [35] or the PU microcapsule (~ 11% for 67 μm) [36], and is attributed to the brittle feature of glass. The normalized maximum strength, σ_{max}, can be calculated from [36]:

$$\sigma_{\max} = \frac{P_{\max}}{\pi((\frac{D_0}{2})^2 - (\frac{D_i}{2})^2)} \approx \frac{P_{\max}}{\pi D_o t} \quad (2)$$

where P_{max} is the maximum load, D_o and D_i are the outer and inner diameter of the HGB, respectively. t is the shell thickness of the HGB. The calculated maximum strength is 12.54 ± 1.98 MPa. Compared with the maximum strength (0.8 ± 0.3 MPa) of the PUF microcapsules with the similar size (65 ± 7 μm) obtained by Keller and Sottos [35], the maximum strength of this etched HGBs is much higher. And it is twice of the maximum strength of the PU microcapsules (~ 6 MPa) with the similar diameter (~ 70 μm) by Yang et al. [36]. These two comparisons verify the robustness of the HGBs after the etching process, although etching through-holes, which can be considered as defects to concentrate the stress, can decrease the strength of the HGBs.

3.3. Characterization of the loaded HGBs

Figure 3a and Figure 3b give the optical microscopic images of the self-healing epoxy thin film located between two glass slides cured for 24 h at RT. The epoxy mixture contains 15 wt% healing agent carriers under ratio of 4 : 1 for HGB-E to HGB-A. The yellow dots in Figure 3a and the bright green dots in Figure 3b are the amine loaded HGBs due to the mixed yellow acid 73, while the white (due to out of focus) or transparent ones in Figure 3a and Figure 3b are the epoxy loaded HGBs. The black patches on some of the HGBs in Figure 3a and the corresponding bright patches in Figure 3b are the empty volumes in the HGBs. From the images, it can be concluded that the HGBs with healants survived from the manufacturing process, and that after 24 h, only few of the HGBs lose the healing agents inside, becoming partially loaded. By counting the numbers of each part shown in the view, the number ratio of HGB-E to HGB-A is about 4 : 1. When considering the density of the loaded healants (1.117 g/cm^3 for the epoxy solution and 0.953 g/cm^3 for the amine solution), the mass ratio of the loaded epoxy to amine is about 4.8 : 1.

3.4. Optimization of the ratio of HGB-E to HGB-A

Due to the two-part feature of this self-healing system, the stoichiometry between the loaded epoxy resin and the loaded amine is of great significance for the self-healing behavior. In order to optimize the self-healing performance, the mass ratio of HGB-E to HGB-A was varied when the total concentration of the two carriers was fixed at 15 wt%. Figure 4a shows the trends of the original peak load, the healed peak load, as well as the healing efficiency with regard to the ratio variation of the two carriers, when the ratio of HGB-E to HGB-A varied from 1 : 1 to 5 : 1. It is observed that the ratio, 4 : 1, possesses the best healing behavior, with healing efficiency of about 62%. Before the optimized ratio, the healed peak load increases steadily while the original peak load slightly falls down, leading to the increasing of the healing efficiency. And after the peak, the healed peak load decreases.

The change of the healing behavior can only be explained by the stoichiometric match for the released two parts at the fracture plane, since the released total healing agents are pretty close to each other during the ratio variation. Based on the result from the optical microscopic images under this composition, the mass ratio of released epoxy resin to released amine is 4.8 : 1. Given the EEW of the loaded epoxy solution (133.05) and the EHW of the loaded amine solution (22.89), theoretically, the best ratio for the epoxy solution and amine solution at free status should be around 5.8 : 1, which is a little higher than the ratio obtained from the experiments. The reasons for the deviation between free status and loaded status, from 5.8 : 1 to 4.8 : 1, lies in three aspects. Firstly, although the HGBs are almost full for both epoxy and amine when incorporated, the evaporation and the leakage from the HGBs for the amine are fast than those for the epoxy due to the relatively higher vapor pressure and the relatively low viscosity for amine solution. Secondly, the functionality of DETA maybe cannot reach as high as 5 due to its small molecule with high functionality. With the progress of the curing process for epoxy by DETA, the mobility of the polymer chain decreases and the reactivity of

the rest active hydrogen on DETA decreases. Considering the relatively low healing temperature (50 °C) and the relatively short chain of DETA molecule, the effective functionality of DETA should be lower than the theoretical functionality. If only four reactive hydrogen atoms take part in the curing process, the ratio of epoxy to amine should be 4.65 : 1, which is very close to the ratio for the loaded epoxy and amine. And lastly, as stated by Selby and Miller [42], moderate excess of amine in the epoxy matrix is beneficial to the fracture toughness of epoxy. The extra amount of amine hardener in 4.8 : 1 may be essential for the relatively higher healing efficiency, defined by recovered mode-I fracture toughness.

3.5. Effect of total concentration on the healing system

The influence of the total concentration of the two healing agent carriers was investigated when the ratio of HGB-E to HGB-A was held at 4 : 1. Figure 4b illustrates the trends of the original peak load, the healed peak load, as well as the healing efficiency, respectively, with respect to the total concentration of the two carriers when the specimens were healed at 50 °C for 24 h. It is observed that a plateau of healing efficiency is formed between 12.5 wt% and 15.0 wt% with height of about 62%. Beyond this plateau, the healing behavior decreases. Before 12.5 wt%, the healed peak load increases sharply while the original peak load only increases steadily and slowly, leading to the rise of the healing efficiency. However, after 15 wt%, the increase of the original peak load is the major change while the healed peak keeps at the similar level, resulting in the decrease of the healing behavior. The reasons for the increase of the healed peak load is that more healing agent can be delivered to the fracture surface, and that the released healing agent only need to diffuse for a shorter distance for better mixing at higher concentration of the healing agent carriers [38].

The influence of the carriers on the original peak load is a little different from the influence of the microcapsule-HGB system in our previous investigation [39]. The original peak load increases steadily to a plateau in this dual HGB system while that in microcapsule-

HGB system goes up exponentially after 10 wt%. In this dual HGB system, the increased fracture toughness can only attributed to the toughening effect of the incorporated healing agent carriers. Compared with the extra stoichiometric mismatch of the matrix introduced by the adhered amine outside the shell of HGBs in the microcapsule-HGB system, the adhered epoxy solution and amine solution can react with each other stoichiometrically in this dual system.

The fractography of the fracture surface was studied on a specimen after it was healed at 50 °C for 24 h. The specimen was incorporated with 15 wt% healing agent carriers at ratio of 4 : 1 for HGB-E to HGB-A. Figure 5a and 5b show the mirrored region of the fracture surface for both sides. As can be seen from the SEM images, most of the etched HGBs are ruptured at the fracture plane and therefore release the healing agent. Attributed to the homogeneous healing feature of the newly formed adhesive film to the fracture surface, cohesive failure of the epoxy film rather than the adhesive failure along the interface occurs during the healing test. It is also observed that not all the fracture surface is wetted by the released healing agent. Figure 5c and 5d show the enlarged area from the mirrored region as indicated by the frames. Some intact HGBs were found at the fracture surface, as indicated by the arrows. By counting the number of the ruptured and the unfractured HGBs, about 8 - 10% of the total HGBs kept intact at the fracture plane. The HGBs with relatively small diameter and thicker shell is difficult to be fractured, especially when they locate too far away from the fracture plane.

3.6. Effect of the healing duration at 50 °C on the healing efficiency

The healing behavior over healing time at 50 °C was also investigated using self-healing specimens containing 15 wt% healing agent carriers in total with ratio 4 : 1 for HGB-E to HGB-A. Figure 4c gives the self-healing efficiency with respect to the healing duration at 50 °C. It is observed that the healing efficiency increases with increased healing time. However, the contribution from the latter added healing time for the healing performance is

much smaller than that from the early stage, especially from the first 3 h. The rising speed gradually decreases with regard to the healing duration. Healing time can influence the healing performance in two aspects. With the increase of healing time, better interdiffusion and therefore better mixing of the two parts can be achieved, since the released two healing agents were not pre-mixed before being released to the crack plane. Besides that, higher molecular weight and cross-linking reaction can be promoted by longer healing time, although too high crosslinking density will deteriorate the fracture toughness.

3.7. Influence of adding carriers on tensile property

As shown in Figure 4a, the incorporation of healing agent carriers is beneficial to the fracture toughness due to the toughening effect of the healing agent carriers. However, the carrier inclusions affect the tensile properties adversely. Figure 6 shows the trends of the tensile strength and elastic modulus with respect to the increase of the total concentration of the two carriers at the optimized ratio. While the modulus is insensitive to the incorporation of the healing agent carriers, the strength was significantly influenced by the carriers. It decreases dramatically by about 18% when 5 wt% was mixed, and then level off at about 65% of the original strength after 10 wt%. The decrease of the tensile strength of the self-healing epoxy can be explained in two aspects. On one hand, the HGBs with solution inside should be treated as defects at the cross-section. And on the other hand, the interface between the inorganic glass shell with the organic epoxy matrix is the weaker area, which also deteriorate the property upon the tensile loading.

4. Conclusions

In this investigation, self-healing epoxy by two-part epoxy-amine chemistry was formulated based on epoxy and amine both carried by etched HGBs. The healing agent carriers were characterized and the healing condition was optimized to achieve higher healing performance:

1. The micro-compression shows that the etched HGBs are much stronger but more brittle than the polymeric PUF or PU microcapsules because of the nature of glass shell.
2. The best healing performance was obtained when the ratio varies to 4 : 1 for HGB-E to HGB-A. Under this ratio, the stoichiometry of the two released healing agents is quite close to that of the theoretical calculation.
3. Highest healing efficiency of about 62 % was achieved at 50 °C for 24 h when 12.5 - 15 wt% healing agent carriers under the optimized ratio was added.
4. The longer the healing time at 50 °C, the higher the healing efficiency. The increased healing efficiency is attributed to the better diffusion for mixing, higher molecular weight, and promoted crosslinkage when treated for a longer time.
5. While the fracture toughness increases with the carrier inclusions, the elastic modulus keeps the same as the pure epoxy and the tensile strength was deteriorated by the incorporated healing agent carriers.

Acknowledgement

The authors greatly acknowledge the financial support from Singapore MoE Tier 1 research fund with grant number of RG17/09 and the Materials Innovation for Marine and Offshore (MIMO) program with the grant numbers of SERC1123004032 under the Agency for Science, Technology and Research (A*Star) of Singapore. It is grateful to Bin Yu and Xin Zhang for their assistance on glass bubble testing and materials preparation.

Reference

[1] Petrie EM. Epoxy Adhesive Formulations. The McGraw-Hill Companies. 2006:87.

[2] White SR, Sottos NR, Geubelle PH, Moore JS, Kessler MR, Sriram SR, et al. Autonomic healing of polymer composites. *Nature*. 2001;409(6822):794-797.

[3] Wu DY, Meure S, Solomon D. Self-healing polymeric materials: A review of recent developments. Prog Polym Sci. 2008;33(5):479-522.

[4] Yang J, Zhang H, Huang M. Emerging technology in aerospace engineering: polymer based self-healing materials. In: Zhang S, Zhao D, editors. Aerospace Materials Handbook: CRC Press; 2012. p. 531-606.

[5] Brown EN, White SR, Sottos NR. Microcapsule induced toughening in a self-healing polymer composite. J Mater Sci. 2004;39(5):1703-1710.

[6] Dry C. Procedures developed for self-repair of polymer matrix composite materials. Compos Struct. 1996;35(3):263-269.

[7] Bleay SM, Loader CB, Hawyes VJ, Humberstone L, Curtis PT. A smart repair system for polymer matrix composites. Compos Pt A-Appl Sci Manuf. 2001;32(12):1767-1776.

[8] Pang JWC, Bond IP. A hollow fibre reinforced polymer composite encompassing self-healing and enhanced damage visibility. Compos Sci Technol. 2005;65(11-12):1791-1799.

[9] Trask RS, Bond IP. Biomimetic self-healing of advanced composite structures using hollow glass fibres. Smart Mater Struct. 2006;15(3):704-710.

[10] Trask RS, Bond IP. Bioinspired engineering study of Plantae vascules for self-healing composite structures. J R Soc Interface. 2010;7(47):921-931.

[11] Williams G, Trask R, Bond I. A self-healing carbon fibre reinforced polymer for aerospace applications. Compos Pt A-Appl Sci Manuf. 2007;38(6):1525-1532.

[12] Trask RS, Williams GJ, Bond IP. Bioinspired self-healing of advanced composite structures using hollow glass fibres. J R Soc Interface. 2007;4(13):363-371.

[13] Therriault D, White SR, Lewis JA. Chaotic mixing in three-dimensional microvascular networks fabricated by direct-write assembly. Nat Mater. 2003;2(4):265-271.

[14] Brown EN, Kessler MR, Sottos NR, White SR. In situ poly(urea-formaldehyde) microencapsulation of dicyclopentadiene. J Microencapsul. 2003;20(6):719-730.

[15] Keller MW, White SR, Sottos NR. A self-healing poly(dimethyl siloxane) elastomer. Adv Funct Mater. 2007;17(14):2399-2404.

[16] Yuan YC, Rong MZ, Zhang MQ, Chen B, Yang GC, Li XM. Self-healing polymeric materials using epoxy/mercaptan as the healant. Macromolecules. 2008;41(14):5197-5202.

[17] Xiao DS, Yuan YC, Rong MZ, Zhang MQ. A Facile Strategy for Preparing Self-Healing Polymer Composites by Incorporation of Cationic Catalyst-Loaded Vegetable Fibers. Adv Funct Mater. 2009;19(14):2289-2296.

[18] Xiao DS, Yuan YC, Rong MZ, Zhang MQ. Hollow polymeric microcapsules: Preparation, characterization and application in holding boron trifluoride diethyl etherate. Polymer. 2009;50(2):560-568.

[19] Wang HP, Yuan YC, Rong MZ, Zhang MQ. Self-Healing of Thermoplastics via Living Polymerization. Macromolecules. 2010;43(2):595-598.

[20] Huang M, Zhang H, Yang J. Synthesis of organic silane microcapsules for self-healing corrosion resistant polymer coatings. Corros Sci. 2012;65(0):561-566.

[21] Huang M, Yang J. Facile microencapsulation of HDI for self-healing anticorrosion coatings. J Mater Chem. 2011;21(30):11123-11130.

[22] Zako M, Takano N. Intelligent material systems using epoxy particles to repair microcracks and delamination damage in GFRP. J Intell Mater Syst Struct. 1999;10(10):836-841.

[23] Tian Q, Yuan YC, Rong MZ, Zhang MQ. A thermally remendable epoxy resin. J Mater Chem 2009;19(9):1289-1296.

[24] Yin T, Rong MZ, Zhang MQ, Yang GC. Self-healing epoxy composites - Preparation and effect of the healant consisting of microencapsulated epoxy and latent curing agent. Compos Sci Technol. 2007;67(2):201-212.

[25] McIlroy DA, Blaiszik BJ, Caruso MM, White SR, Moore JS, Sottos NR. Microencapsulation of a Reactive Liquid-Phase Amine for Self-Healing Epoxy Composites. Macromolecules. 2010;43(4):1855-1859.

[26] Li Q, Mishra AK, Kim NH, Kuila T, Lau K-t, Lee JH. Effects of processing conditions of poly(methylmethacrylate) encapsulated liquid curing agent on the properties of self-healing composites. Compos Pt B-Eng. 2013;49(0):6-15.

[27] Jin H, Mangun CL, Stradley DS, Moore JS, Sottos NR, White SR. Self-healing thermoset using encapsulated epoxy-amine healing chemistry. Polymer. 2012;53(2):581-587.

[28] Jin H, Mangun CL, Griffin AS, Moore JS, Sottos NR, White SR. Thermally Stable Autonomic Healing in Epoxy using a Dual-Microcapsule System. Adv Mater. 2013;10.1002/adma.201303179.

[29] Pang JWC, Bond IP. 'Bleeding composites' - damage detection and self-repair using a biomimetic approach. Compos Pt A-Appl Sci Manuf. 2005;36(2):183-188.

[30] Williams GJ, Bond IP, Trask RS. Compression after impact assessment of self-healing CFRP. Compos Pt A-Appl Sci Manuf. 2009;40(9):1399-1406.

[31] Yin T, Zhou L, Rong MZ, Zhang MQ. Self-healing woven glass fabric/epoxy composites with the healant consisting of micro-encapsulated epoxy and latent curing agent. Smart Mater Struct. 2008;17(1).

[32] Williams HR, Trask RS, Bond IP. Self-healing composite sandwich structures. Smart Mater Struct. 2007;16(4):1198-1207.

[33] Williams HR, Trask RS, Bond IP. Self-healing sandwich panels: Restoration of compressive strength after impact. Compos Sci Technol 2008;68(15-16):3171-3177.

[34] Yin T, Rong MZ, Wu J, Chen H, Zhang MQ. Healing of impact damage in woven glass fabric reinforced epoxy composites. Compos Pt A-Appl Sci Manuf. 2008;39(9):1479-1487.

[35] Keller MW, Sottos NR. Mechanical properties of microcapsules used in a self-healing polymer. Exp Mech. 2006;46(6):725-733.

[36] Yang JL, Keller MW, Moore JS, White SR, Sottos NR. Microencapsulation of Isocyanates for Self-Healing Polymers. Macromolecules. 2008;41(24):9650-9655.

[37] Zhang H, Yang J. Etched glass bubbles as robust micro-containers for self-healing materials. J Mater Chem A. 2013;10.1039/c3ta13227g.

[38] Zhang H, Yang J. Development of Self-healing Polymers via Amine-Epoxy Chemistry Part I: Properties of Healing Agent Carriers and Modelling of Two-Part Self-Healing System. submitted to Smart Mater Struct.

[39] Zhang H, Yang J. Development of Self-Healing Polymers via Amine-Epoxy Chemistry. Part II: Systematical Evaluation of Self-Healing Performance. Smart Mater Struct.

[40] Axson North America I. Materials Safety Data Sheet for Epolam 5015 resin. 2009.

[41] Brown EN, Sottos NR, White SR. Fracture testing of a self-healing polymer composite. Exp Mech. 2002;42(4):372-379.

[42] Selby K, Miller LE. Fracture toughness and mechanical behaviour of an epoxy resin. J Mater Sci. 1975;10(1):12-24.

Figure captions

Figure 1 (a) Overview with the cross-section of the original HGBs; (b) Surface morphology of the original HGBs; (c) Overview with the cross-section (inset at top right) and a typical enlarged etched HGB (inset at bottom right); and (d) Microscopic image of the etched HGBs.

Figure 2 (a) Digital image and scheme of the micro-compressive testing process; (b) Typical Load-Displacement curve of the etched HGB.

Figure 3 Optical microscopic images of the loaded HGBs separately with epoxy and amine solution after their incorporation into epoxy matrix under 80 % intensity of the light source (a) and 10% intensity of the light source (b), respectively.

Figure 4 (a) and (b) Original peak load, healed peak load, as well as healing efficiency of the specimen with regard to the ratio variation of HGB-E to HGB-A when the total concentration was held at 15 wt% and the total concentration of the dual carriers at the optimized ratio, respectively;(c) Healing efficiency with respect to the healing duration at 50 °C.

Figure 5 (a) and (b) Fracture surface for both sides of the self-healing specimen with 15 wt% healing carriers at the optimized ratio after healing at 50 °C for 24 h. (c) and (d) Enlarged areas in (a) and (b), respectively.

Figure 6 Trend of tensile strength and modulus regarding the total carrier concentration.

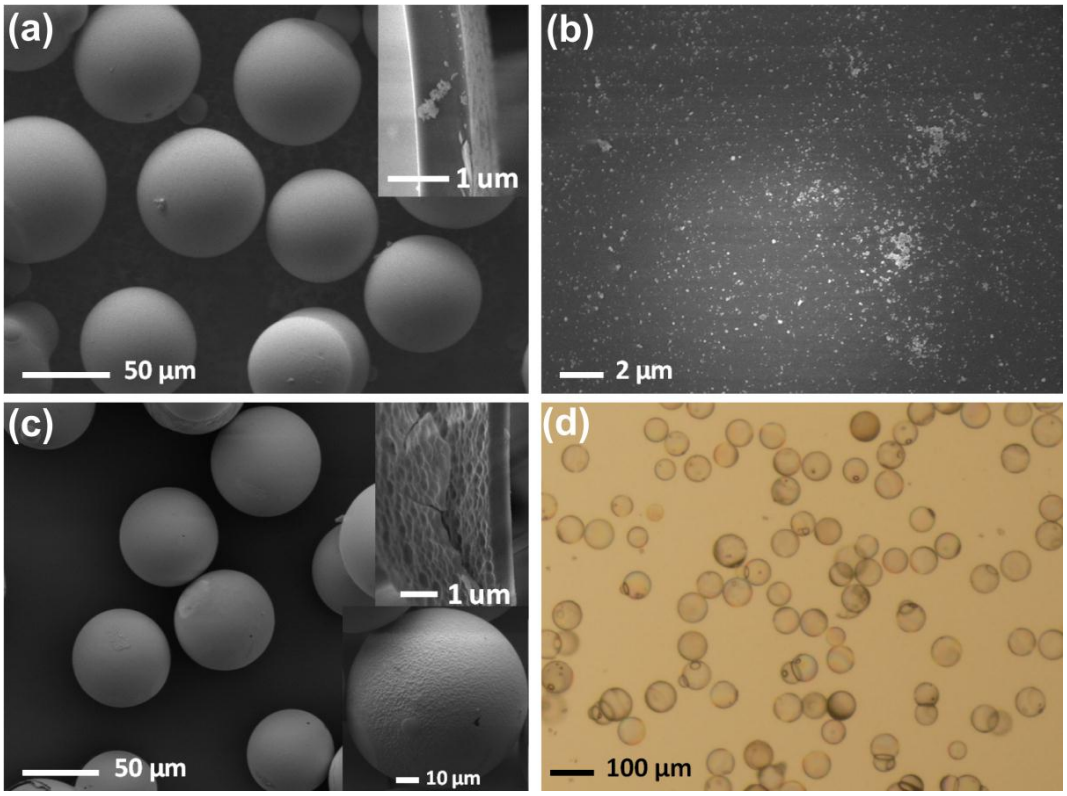

Figure 1

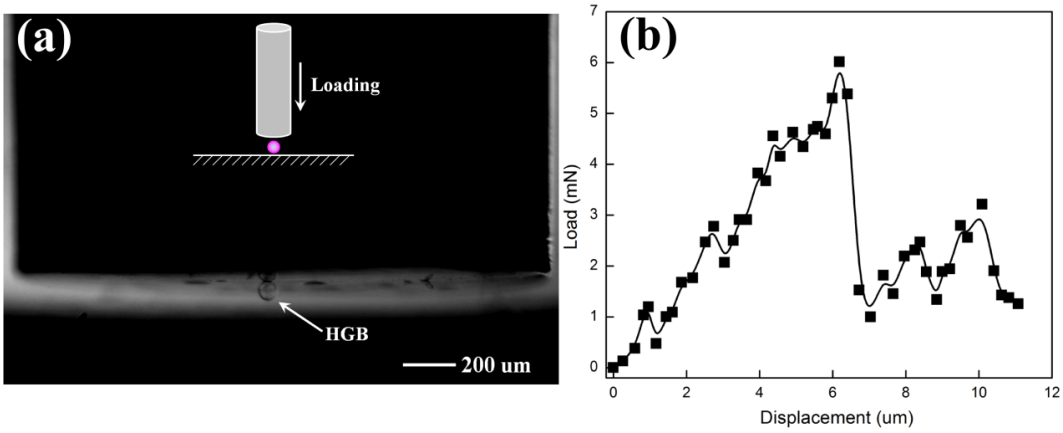

Figure 2

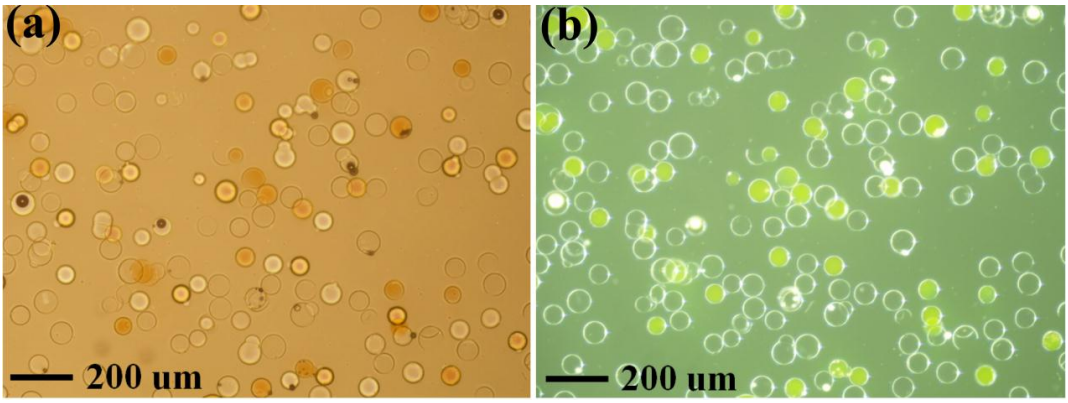

Figure 3

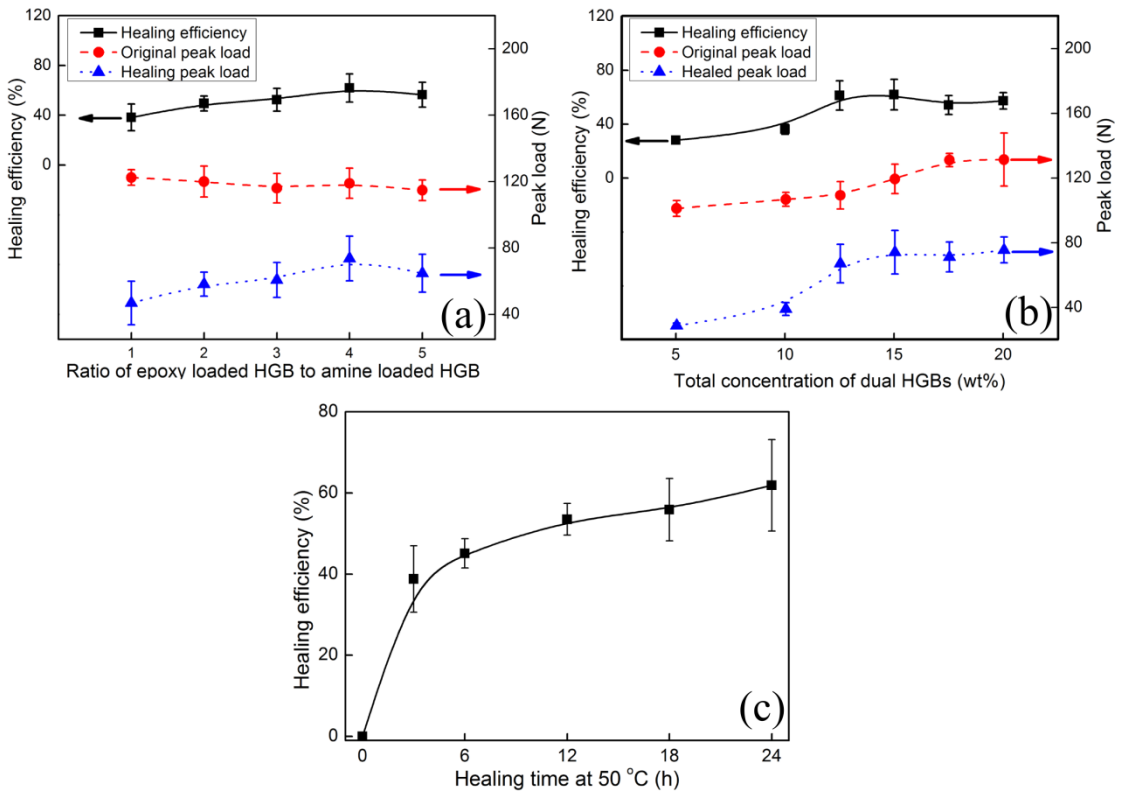

Figure 4

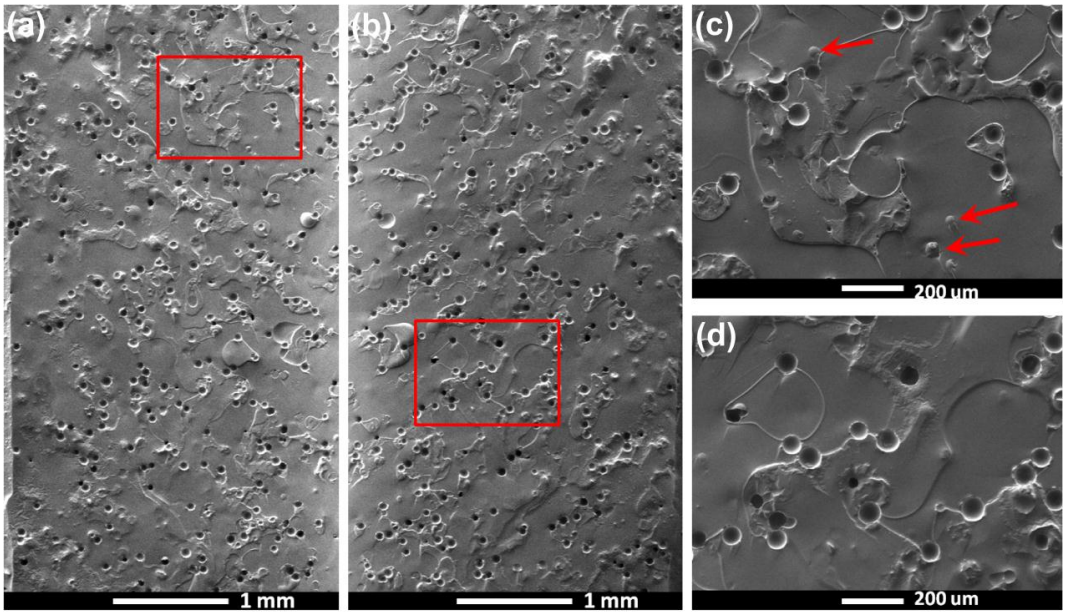

Figure 5

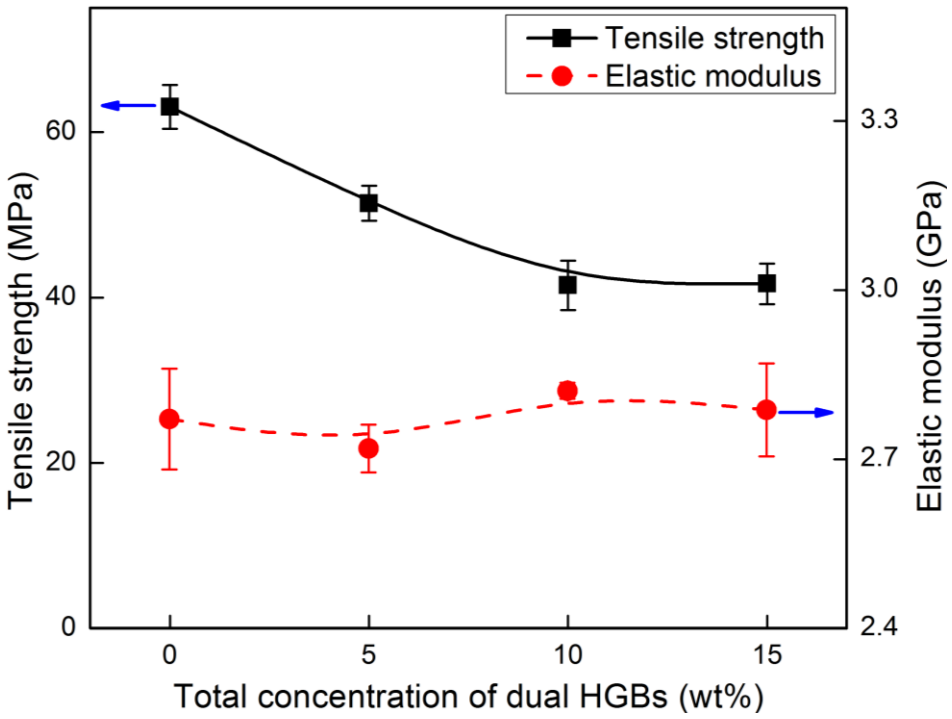

Figure 6